

Title	Ultrasonic focusing using a stacked thin-plate region
Author(s)	Fukuchi, Takaaki; Hayashi, Takahiro; Mori, Naoki
Citation	Japanese Journal of Applied Physics. 2023, 62, p. SJ1005
Version Type	AM
URL	https://hdl.handle.net/11094/92342
rights	This Accepted Manuscript is available for reuse under a CC BY-NC-ND licence after the 12 month embargo period provided that all the terms of the licence are adhered to
Note	

Osaka University Knowledge Archive : OUKA

<https://ir.library.osaka-u.ac.jp/>

Osaka University

Ultrasonic focusing using a stacked thin-plate region

Takaaki Fukuchi, Takahiro Hayashi* and Naoki Mori

Department of Mechanical Engineering, Graduate School of Engineering, Osaka University

E-mail: hayashi@mech.eng.osaka-u.ac.jp

This paper describes a stacked thin-plate region for focusing the transmitted waves. The region was designed to focus the wave field in the bulk medium by utilizing the dispersion nature of Lamb waves. The first numerical calculation proved that an incident plane wave changes the wavefront in a stacked thin-plate region because of the different phase velocities in plates with different thicknesses, and the resulting transmitted wave was focused at the target. Second, when a delayed longitudinal wave was applied to the edge of the stacked thin - plate region with identical thickness, the numerical calculations showed that the delayed wavefront of the S_0 mode was preserved in the stacked plate region, and that the transmitted longitudinal wave was appropriately focused at the target. The focusing devise consisting of a stacked thin-plate structure is useful for the buffer for phased array inspection.

1. Introduction

Ultrasonic waves in isotropic elastic media propagate at different velocities in two vibration modes: longitudinal and transverse waves. If surfaces or interfaces exist, ultrasonic waves propagate in various forms such as reflection, refraction, and diffraction. They are widely used in acoustic devices and non-destructive inspections by artificially controlling the propagation of ultrasonic waves and providing their functionality. For example, surface acoustic wave (SAW) devices efficiently propagate Rayleigh waves by preparing comb-like electrodes on the surface of a piezoelectric substrate with spacing corresponding to the wavelength of the surface waves. SAW devices are widely used as band-pass filters¹⁾ and sensors due to their narrowband characteristics.²⁾ In addition, classical normal-beam and angle-beam transducers were designed to obtain the desired ultrasonic wave propagation by selecting the element size and wedge angle that determine the directivity and refraction angle of the ultrasonic wave in the solid.³⁾

Recently, various researches have been conducted on functional materials that can control desired sound waves using artificial structures consisting of aggregates of scatterers and resonators, called metamaterials and metasurfaces. For example, a characteristic sound wave can be designed by controlling the bandgap of sound waves using a periodic structure called a phononic crystal.⁴⁻⁸⁾ Moreover, new ultrasonic wave propagation has been realized by acoustic diodes that transmit sound waves in one direction,⁹⁻¹²⁾ acoustic cloaking devices that allow sound waves to go around without being reflected,^{13, 14)} and efficient sound absorbers,¹⁵⁻¹⁸⁾ and their applications are being researched.

However, the functionality and characteristics of an aggregate of scatterers in acoustic metamaterials and metasurfaces are not predictable from the wave theory for an individual scatterer. Therefore, band gap analyses based on Bloch's theorem for periodic structures and numerical simulations are necessary to obtain efficient functionalities. Moreover, the authors have focused on a stacked thin-plate structure in which ultrasonic wave propagation can be controlled with the prediction from the theory of Lamb waves in a thin plate. The numerical analysis of wave propagation in the periodic stacked thin-plate structure revealed that the structure changes the direction of the transmitted transverse wave, as predicted theoretically.¹⁹⁾ In addition, numerical simulations¹⁹⁾ revealed that transverse waves can be controlled by using stacked thin-plate regions with different thicknesses.²⁰⁾ In this study, we examined

ultrasonic wave focusing using a stacked thin-plate structure.

Ultrasonic wave focusing can be achieved using spherical or cylindrical piezoelectric films such as polyvinylidene fluoride (PVDF) or piezoelectric ceramics such as lead zirconate titanate (PZT), and is widely used in ultrasonic microscopes.²¹⁾ In phased array technology, ultrasonic energy can be focused at a desired point in living bodies and solid materials by applying pulse signals with different delays to multiple piezoelectric elements, and the internal image can be obtained by moving the focal position. Phased array imaging has long been used for medical diagnosis and is widely used in various industrial fields.²²⁾⁻²⁷⁾

This study investigates transverse- and longitudinal-wave focusing in an elastic medium by controlling the wave field propagating in a stacked thin-plate region using the characteristics of Lamb waves in thin plates, which can be theoretically predicted from the dispersion curves.

2. Ultrasonic focusing using a stacked plate region with different thickness

2.1 Designing combination of plates

First, we considered ultrasonic focusing with a stacked plate structure consisting of plates of different thicknesses. Figure 1 shows the phase velocity dispersion curve and wave structures for an aluminum alloy plate with longitudinal and transverse wave velocities of 6400 and 3170 m/s, respectively, which will also be used in later calculations.²⁸⁻³⁰⁾ The horizontal axis of the dispersion curve is expressed as the product of frequency f and plate thickness d . The wave structures represent the displacement distribution of the plate thickness cross-section of length $10d$ at points (a)–(d) in the dispersion curve. The grid shift in the cross-section indicates the displacement. The shade of the cross-section indicates the displacement in the dominant vibration direction, which is the plate thickness direction in (a) and (b) and the propagation direction in (c) and (d), respectively. In (a) and (c), $fd = 0.5$ MHz mm, and in (b) and (d), $fd = 1.0$ MHz mm. Since both are below the cutoff frequency of the A1 mode, only the A0 and S0 modes exist as propagation modes in the low fd band. From these wave structures, both dominant displacement distributions were almost uniform over the plate thickness in the low fd band.

In addition, as seen in the phase velocity dispersion curve, Lamb waves have a dispersion nature, in which the phase velocity changes with fd . The phase velocity of the A0 mode changes significantly with fd , particularly in this low fd band. In this section, we consider the ultrasonic focusing using this property. Figure 2 shows a schematic of the focusing with a stacked plate region consisting of thin plates of different thicknesses, where a dynamic force at the same phase is applied in the vertical direction on the left edge of the region. This corresponds to the case in which the shear-wave transducer was attached to the left end of the stacked plate region. In this case, the A0 mode of the Lamb wave, in which the vertical flexural vibration is dominant, propagates in each thin plate. For a stacked plate region with different thicknesses, the phase differences increase as they travel in the thin plates. Since the A0 mode in this low fd region has an almost uniform wave structure in the plate thickness direction, it can be considered that the transverse wave oscillator with delay is placed at the right end of the thin plate. Therefore, transverse waves propagating in the object on the right can be focused by appropriately controlling the phase difference, i.e., by designing the length and thickness of each thin plate.

Subsequently, a specific design for the stacked thin-plate region is described. Although it follows the focal law in phased-array ultrasonic focusing,²²⁻²⁷⁾ it differs in unequal thickness. As shown in Fig. 3, the thickness of the central plate in the stacked structure is d_0 , and the length is L . The center at the right edge of the stacked region is defined as the origin $(x_0, y_0) = (0, 0)$, and the coordinates of the focal point are (x_f, y_f) , $(x_f > 0)$. Then, the distance R_0 from the origin to the focal point, and the distance R_i from the center coordinates of the i^{th} thin plate $(0, y_i)$ to the focal point, can be expressed as

$$R_i = \sqrt{x_f^2 + (y_i - y_f)^2}, R_0 = \sqrt{x_f^2 + y_f^2}. \quad (1)$$

where the y position of the center of the i^{th} thin plate is expressed by the following equations if all gaps between the plates are assumed to be 0.

$$y_i = \frac{d_0}{2} + \sum_{m=1}^{i-1} d_m + \frac{d_i}{2} \text{ for } i > 0, \quad (2)$$

$$y_i = -\frac{d_0}{2} - \sum_{m=-1}^{i-1} d_m - \frac{d_i}{2} \text{ for } i < 0.$$

To focus the transmitted transverse wave, the traveling time when it propagates in the i^{th} thin plate in the A0 mode and reaches the focal point as a transverse wave should be the same as that when it passes through the 0th thin plate and reaches the focal point. Therefore, the phase velocity c_i of the i^{th} thin plate, that is, the thickness d_i of the i^{th} thin plate, is determined to satisfy the following equation:

$$\frac{L}{c_i} + \frac{R_i}{c_T} = \frac{L}{c_0} + \frac{R_0}{c_T}. \quad (3)$$

When the product of the frequency and plate thickness fd exceeds $fd = c_T/2$, the A1 mode appears as a propagation mode, and the wave structure of the A0 mode cannot be approximated uniformly in the plate thickness direction. Therefore, the time difference was adjusted by adding an integral multiple of period $1/f$ to the time delay. That is, the plate thickness d_i was determined as

$$\frac{L}{c_i} + \frac{R_i}{c_T} + \frac{n}{f} = \frac{L}{c_0} + \frac{R_0}{c_T}, \quad (4)$$

where n represents an integer.

When the frequency, region length, and central plate thickness were $f = 1$ MHz, $L = 20$ mm, and $d_0 = 0.400$ mm, respectively, the stacked region consisting of 111 thin plates was designed to focus the transmitted waves at $(x_f, y_f) = (20 \text{ mm}, 0 \text{ mm})$. Figure 4 shows the thickness combination of the region where the central plate number is zero and the symmetric structure $d_{-i} = d_i$ ($i = 1, 2, \dots, 55$) because of the focus point on the centerline. The total thickness of the region consisting of these 111 layers results in 74.15 mm. The horizontal axis shows the plate number and the vertical axis shows the thickness d_i mm. The thickness increases monotonically from the 0th plate to the 44th plate. However, the thickness decreases at the 45th, 48th, 51st, and 55th plates, according to Eq. (4).

Transverse wave focusing in a stacked plate region using the A0 mode is described above. The focusing idea can also be applied to the longitudinal wave by using the S0 mode in the plates and focusing the longitudinal wave in the object on the right. Although the S0 mode in the low fd band exhibits an almost uniform wave structure within the plate thickness, the distance of the plate region must be long in order to obtain the desired phase difference

at the right end of the stacked plate region due to the small dispersion of the S0 mode.

2.2 Ultrasonic focusing with velocity dispersion of A0 mode

The above idea is confirmed in this section by performing numerical simulations using COMSOL Multiphysics®. First, the focusing of the transverse waves using thin plates with different thicknesses was verified. The calculation region is illustrated in Fig. 5. Although the upper and lower surfaces of the adjacent thin plates overlapped, both were under a traction-free boundary condition. A vertical dynamic traction force was applied to the left edge of the plate region at a center frequency of 1 MHz. The wave traveling in the stacked plate region is transmitted through the right bulk medium. An absorbing boundary was provided at the end of the bulk medium to prevent reflected waves. All calculations in this study were two-dimensional under plane strain conditions. The calculation region was divided into square cells with a maximum length of 0.25 mm. The stacked region and the object on the right side were assumed to be the same aluminum alloy with longitudinal and transverse wave velocities of 6400 m/s and 3170 m/s, respectively, and a density of 2700 kg/m³, and were connected under a continuous boundary condition.

Figure 6 shows the wave propagation when the A0 mode reaches the boundary between the plate region and the right bulk region after applying a vertical dynamic force in the same phase at the left end of the stacked plate region. To express the component of the transverse wave, the rotation of the displacement vector \mathbf{u} is represented in color, which is normalized by the maximum value at this moment. Figure 6 (a) shows the wave propagation when the entire left end is excited in phase; Fig. 6 (b) represents when the center is excited in the range of $-15 \text{ mm} \leq y \leq 15 \text{ mm}$, and Fig. 6 (c) represents the wave propagation when a part of the lower portion is excited in the range of $-30 \text{ mm} \leq y \leq 0$. In all cases, as it propagates, an arc-shaped wavefront is formed by the difference in phase velocity within the stacked plate region, and the wavefronts at the exit of the stacked plate region become an arc centered at the focal point.

Figure 7 shows the calculation results of the wave propagation after propagating to the bulk medium on the right, plotting the maximum value of the rotation of the displacement vector \mathbf{u} over the entire calculation time. Figures 7 (a)–(c) show the calculation results under the incident conditions shown in Figs. 6 (a)–(c). In all cases, the wave propagated

appropriately toward the desired focal point. Figure 7 (a) represents a very sharp focus at the focal position with a large aperture angle, and Figs. (b) and (c) represent a wave field with a small aperture angle that extends long before and after the focal point. This is identical to the findings of phased-array ultrasonic focusing. Moreover, Fig. 7 (c) shows that focusing is possible even if the focal point is not under the transducer. In addition, if we consider wave propagation in the opposite direction, this stacked-plate region can be regarded as a structure that converts cylindrical waves into plane waves. Therefore, ultrasonic emission can be converted into a plane wave and used as energy with a flat piezo element by contacting the structure onto the surface of the object with a sound source at a fixed position.

2.3 Ultrasonic focusing with velocity dispersion of S0 mode

Since the A0 mode has a large velocity dispersion with respect to the plate thickness, a phase difference occurs within a short region length L . As mentioned in Sect. 2.1, an extended stacked plate region is required to focus the longitudinal wave using the S0 mode with a relatively small dispersion. The longitudinal wave was designed to focus on $(x_f, y_f) = (20 \text{ mm}, 0 \text{ mm})$ with a region length $L = 270 \text{ mm}$, frequency 1 MHz, and central plate thickness $d_0 = 1.000 \text{ mm}$. Figure 8 shows the combinations of thicknesses of the 41 thin plates used for focusing. Since the target is located at the centerline, $d_{-i} = d_i$ ($i = 1, 2, \dots, 20$) as in Fig. 4.

Figure 9 shows the divergence of the displacement vector \mathbf{u} in the transmission region in color, which represents the longitudinal wave propagation. As shown in Fig. 7, the maximum value at each position over the entire time range was acquired as an intensity distribution, and the values normalized by the maximum value are shown in color. The cross mark is the focusing target, and focusing is achieved as expected.

3. Ultrasonic focusing using a stacked plate region with identical thickness

3.1 Ultrasonic focusing by time delay in a stacked plate region with identical thickness

As mentioned in Sect. 2.1, the S0 mode has a small dispersion in the low fd band. It has the advantage of a small waveform distortion in propagation, even for pulsed

broadband waves. In other words, the S_0 mode incident from one edge propagates through the thin plate while maintaining the form of the pulsed wave and excites waves at the object contacting the other plate end. This wave propagation in a stacked plate region implies that it works as an ideal delay line and can be used as a buffer material for focusing by combining it with a phased array transducer. Here, for simplicity, we consider a stacked plate region consisting of thin plates of identical thickness.

Figure 10 shows a schematic diagram of the longitudinal wave focusing using a stacked plate region and time-delayed incident waves at the left end. When a longitudinal wave is incident from the left end of the stacked region, the S_0 mode of the Lamb wave, whose propagation and vibration directions are the same, travels through each thin plate. In the low fd band, only the S_0 mode, which is dominated by longitudinal vibration, can propagate. S_0 mode can propagate over long distances without waveform distortion due to the small dispersion nature. These waveforms propagate with equal phase velocities because all the thin plates have the same thickness. Therefore, when a delay is given to the incident waves applied to each thin plate in the same manner as the phased-array transducer, the delay is maintained and transmitted to the other edge of the stacked region. This means that ultrasonic focusing is feasible as in an ordinary phased array inspection where the phased-array transducer is directly attached. Strictly speaking, the focusing performance is expected to be slightly lower when the phased array is attached directly because of the small dispersion and reflection at the edges of the stacked region.

3.2 Results for a stacked plate region with identical plate thickness

In this section, ultrasonic focusing using a stacked plate region consisting of thin plates of identical thickness and time-delayed incident waves are presented using numerical simulations. The aluminum alloy was assumed to be used in the previous section. The distance between the thin plates was assumed to be zero in the previous section, but a small gap was set between the plates, assuming that the linear phased-array transducer consisting of multiple piezoelectric elements with small gaps was installed at the left end of the structure. As a phased array transducer, we assumed a linear array transducer with a total width of 29.8 mm for the excitation region, a width of 0.8 mm for each element, a gap of 0.2 mm between elements, and 30 elements. As shown in Fig. 11, each thin plate in the stacked

plate region is attached to one element of the linear array transducer and has a length of 100 mm. In the numerical calculation, at the left end of the stacked plate region, a surface force with a central frequency of 1 MHz was applied perpendicular to the plate edge surface, and the S0 mode was excited in the thin plate. The incident wave on each edge of the thin plate was given a delay to focus at $(x_f, y_f) = (20 \text{ mm}, 0 \text{ mm})$ by the calculation using the focal law. As shown in Fig. 3, the center of the right edge of the stacked region was the coordinate origin.

Figure 12 shows the calculation results for focusing when using the stacked-plate region. The maximum value of the divergence of the displacement vector \mathbf{u} at each position over the entire time range is shown in color, which indicates that longitudinal wave propagation is displayed. It is normalized by the maximum value in Fig. 12, and it can be observed that this maximum value approximately agrees with the focusing target, as indicated by the cross mark at $(x, y) = (20 \text{ mm}, 0 \text{ mm})$.

This result shows that the stacked plate region works effectively as a buffer material when a distance between the phased array transducer and the target object is required. For example, a hot targeted object and a small accessible space where a large phased array transducer cannot be inserted. Figure 13 (a) shows the wave field distribution when the phased-array transducer is brought into direct contact with the object, while Fig. 13 (b) shows the wave field distribution when a uniform thick plate of the same length is used as a homogeneous buffer material for comparison, demonstrating this effect. Both figures show values normalized by the highest value. Figure 13 (a) shows almost the same wave field distribution as in Fig. 12, which proves that the buffer material in the stacked plate region in Fig. 12 shows very effective focusing. Figure 13 (b) shows no focusing, and the overall intensity is small. This is because the buffer material reduces the aperture of the ultrasonic transducer, and the reflection from the wall surface in the homogeneous buffer region has an undesirable effect.

Furthermore, we investigated the focusing performance at different positions because it is important in practical applications to focus ultrasonic waves at arbitrary positions as well as in the axial direction. Focusing at $(x_f, y_f) = (30 \text{ mm}, 20 \text{ mm})$ was examined by readjusting the delay time of the applied surface force. Figures 14 (a) and 14

(b) show the wave field distribution using the same representation as that in Figs. 12 and 13. The cross mark represents the focal position $(x_f, y_f) = (30 \text{ mm}, 20 \text{ mm})$. The result was almost identical to that obtained using the linear array transducer. Accordingly, it was shown that a stacked plate region composed of thin plates with the same thickness is effective as a buffer structure for the linear array transducer.

As proposed in this chapter, the stacked thin-plate region of equal thickness can be applied to non-destructive inspection in a high-temperature environment. Since large factories, such as nuclear power plants, operate at temperatures of several hundred degrees or more, it is necessary to use a probe that can withstand high temperatures or a buffer rod as a thermal buffer to reduce the effect on the transducer.³¹⁻³³⁾ However, as shown in Fig. 13(b), when using the conventional buffer rod and phased-array probe, the distance between the incident position and the focal point is too long to focus. Focusing can be achieved using a buffer rod consisting of thin plates in the same way that a phased array can be attached directly to the inspected object. It was also possible to transmit waves to arbitrary positions using this focusing method by controlling the delay at the time of incidence. Therefore, it is expected to be used as a new tool for imaging the internal defects of an inspected object by electronically scanning ultrasonic waves.

4. Conclusions

We proposed two ultrasonic focusing techniques using a stacked thin-plate region. First, we described the dispersion nature of the A0 and S0 modes of Lamb waves in the low fd band and demonstrated the ultrasonic focusing technique using a stacked plate region with different thicknesses. Numerical calculations showed that a phase difference occurred when the incident transverse and longitudinal waves of the same phase propagated through the region as Lamb waves. As a result, the transmitted wave was focused at the target. Second, we demonstrated a method of ultrasonic focusing using a stacked plate region with the same thickness, and it was shown that the longitudinal wave could be focused by delaying the incident wave on each thin plate. The focusing performance when using the proposed region was equivalent to focusing without a buffer using the phased array transducer. Moreover, the stacked thin-plate region enabled us to focus on a distance that could not be focused using

conventional buffer rods. Therefore, a stacked thin-plate region is expected to be applied in fields where phased-array transducers cannot be attached directly, such as non-destructive inspection of high-temperature objects.

Acknowledgments

This study was partially supported by the Japan Society for the Promotion of Science KAKENHI [grant number 21H01573].

References

- 1) C. K. Campbell, *Surface Acoustic Wave Devices for Mobile and Wireless Communication*, (Academic Press, San Diego, 1998).
- 2) D. S. Ballantine, R. M. White, S. J. Martin, A. J. Ricco, E. T. Zellers, G. C. Frye, and H. Wohltjen, *Acoustic wave sensors, Theory, design, and physico-chemical applications*, (Academic Press, San Diego, 1997).
- 3) J. Krautkramer, H. Krautkramer, *Ultrasonic Testing of Materials*, (Springer Verlag, 1990)
- 4) N. Fang, D. Xi, J. Xu, M. Ambati, W. Srituravanich, C. Sun, and X. Zhang, *Nat. Mater.* **5**, 452 (2006).
- 5) S. K. Lee, B. R. Mace, and M. J. Brennan, *J. Sound Vib.* **304**, 31 (2007).
- 6) Y. Pennec, J. O. Vasseur, B. Djafari-Rouhani, L. Dobrzyński, and P. A. Deymier, *Surf. Sci. Rep.* **65**, 229 (2010).
- 7) M. Maldovan, *Nature* **503**, 209 (2013).
- 8) R. P. Moiseyenko, S. Herbison, N. F. Declercq, and V. Laude, *J. Appl. Phys.* **111**, 034907 (2012).
- 9) X.-F. Li, X. Ni, L. Feng, M.-H. Lu, C. He, and Y.-F. Chen, *Phys. Rev. Lett.* **106**, 084301 (2011).
- 10) H. X. Sun, S. Y. Zhang, and X. J. Shui, *Appl. Phys. Lett.* **100**, 103507 (2012).
- 11) X. P. Wang, L. L. Wan, T. N. Chen, Q. X. Liang, and A. L. Song, *Appl. Phys. Lett.* **109**, 044102 (2016).
- 12) Y. F. Zhu, X. Y. Zou, B. Liang, and J. C. Cheng, *Appl. Phys. Lett.* **107**, 113501 (2015).
- 13) N. Boechler, G. Theocharis, and C. Daraio, *Nat. Mater.* **10**, 665 (2011).
- 14) H. Chen and C. T. Chan, *J. Phys. D* **43**, 113001 (2010).
- 15) K. Watanabe, M. Fujita, and K. Tsuruta, *Jpn. J. Appl. Phys.* **59**, SKKA06 (2020).
- 16) S. Takasugi, K. Watanabe, M. Misawa, and K. Tsuruta, *Jpn. J. Appl. Phys.* **60**, SDDA01 (2021).
- 17) X. Peng, J. Ji, and Y. Jing, *J. Acoust. Soc. Am.* **144**, EL255 (2018).
- 18) C. Chen, Z. Du, G. Hu, and J. Yang, *Appl. Phys. Lett.* **110**, 221903 (2017).
- 19) T. Fukuchi, N. Mori and T. Hayashi, *Jpn. J. Appl. Phys.* **61**, SG1048 (2022).
- 20) T. Fukuchi, T. Hayashi, and N. Mori, *Proc. of Symp. on Ultrasonics Electronics*, (USE2022) **43**, 3Pa1-4.

- 21) N. Chubachi, J. ichi Kushibiki and T. Sannomiya, *Jpn. J. Appl. Phys.* **20**, 73 (1981).
- 22) W. Lee and Y. Roh, *Biomed. Eng. Lett.* **7**, 91 (2017).
- 23) B. W. Drinkwater and P. D. Wilcox, *NDT E Int.* **39**, 525 (2006).
- 24) S. J. Song, H. J. Shin and Y. H. Jang, *Nucl. Eng. Des.* **214**, 151 (2002).
- 25) J. Yen and S. W. Smith, *IEEE Trans Ultrason Ferr Freq Cont.* **51**, 216 (2004).
- 26) Y. Ohara, H. Nakajima, S. Hauptert, T. Tsuji and T. Mihara, *Jpn. J. Appl. Phys.* **59** SKKB01 (2020).
- 27) Y. Ohara, M. C. Remillieux, T. J. Ulrich, S. Ozawa, K. Tsunoda, T. Tsuji and T. Mihara, *Jpn. J. Appl. Phys.* **61** SG1044 (2022).
- 28) K. F. Graff, *Wave Motion in Elastic Solids* (Dover Publications, New York, 1991), p. 431
- 29) L. W. Schmerr Jr, *Fundamentals of Ultrasonic Nondestructive Evaluation: A Modeling Approach* (Plenum Press, New York, 1998), p. 141
- 30) T. Hayashi and K. Kawashima, *Ultrasonics* **40**, 193 (2002).
- 31) C. K. Jen, J. G. Legoux and L. Parent, *NDT E Int.* **33**, 145 (2000).
- 32) D. Burhan, I. Ihara and Y. Seda, *Mater. Trans.* **46**, 2107 (2005).
- 33) F. M. Foudzi and I. Ihara, *J. Phys. Conf. Ser.* **520**, 1 (2014).

Figure Captions

Fig. 1. Phase velocity dispersion curves and wave structures for A0 and S0 modes in the low fd band.

Fig. 2. Ultrasonic focusing in the bulk region after Lamb waves travel through plates with different thickness.

Fig. 3. Coordinates of a stacked plate region and the focal point from the calculations.

Fig. 4. Thickness combination for transverse wave focusing.

Fig. 5. Calculation region for focusing of transverse wave at the center of the bulk region.

Fig. 6 Wave propagation in a stacked plate region. The surface color is the magnitude of $\text{rot } \mathbf{u}$. The cross mark is the focusing point.

Fig. 7 Wave field for transverse wave focusing with different thickness plates. The color denotes maximum values of $\text{rot } \mathbf{u}$ over the whole time range. The cross mark is a focusing target.

Fig. 8 Thickness combination for longitudinal wave focusing.

Fig. 9 Wave field for longitudinal wave focusing with different thickness plates. The color denotes maximum values of $\text{div } \mathbf{u}$ over the whole time range. The cross mark is a focusing target.

Fig. 10 Ultrasonic focusing using plates with identical thickness and time delay.

Fig. 11 Relation between linear phased array and stacked plate region.

Fig. 12 Wave field for focusing with identical thickness plates and time delayed incident waves. The color denotes maximum values of $\text{div } \mathbf{u}$ over the whole time range.

Fig. 13 Wave field for focusing (a) without a buffer material and (b) an ordinary homogeneous buffer material.

Fig. 14 Wave field for focusing at the off-center of the bulk region.

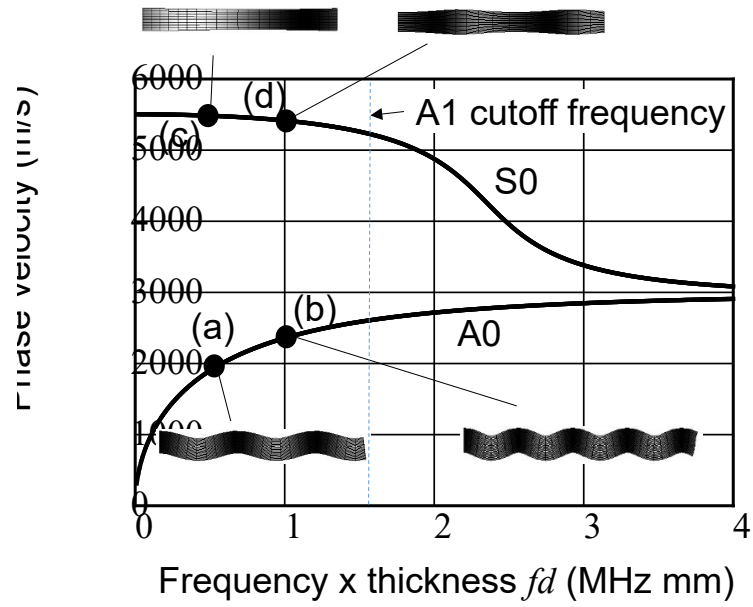


Fig. 1 Phase velocity dispersion curves and wave structures for A0 and S0 modes in the low fd band

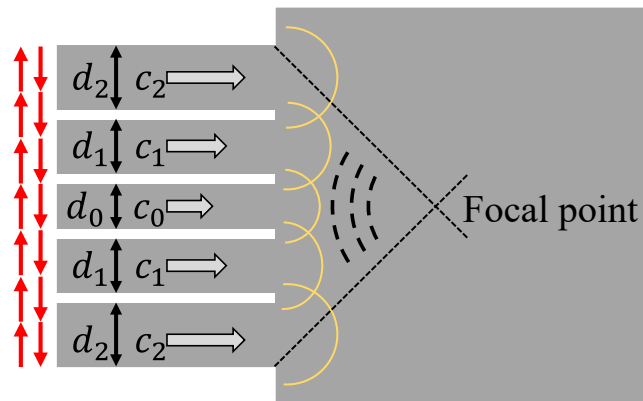


Fig. 2 Ultrasonic focusing in the bulk region after Lamb waves travel through plates with different thickness

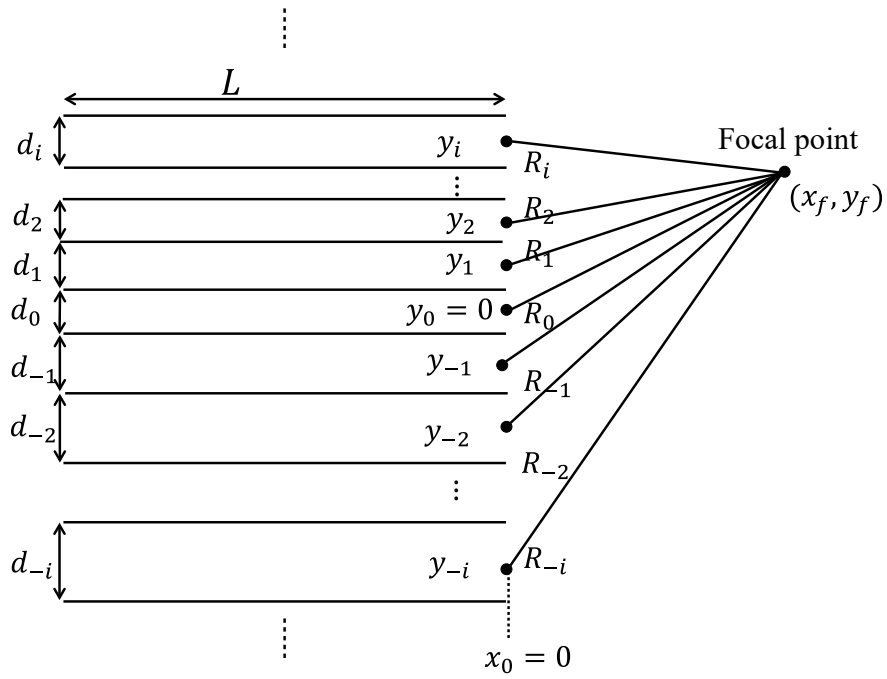


Fig. 3 Coordinates of a stacked plate region and the focal point from the calculations

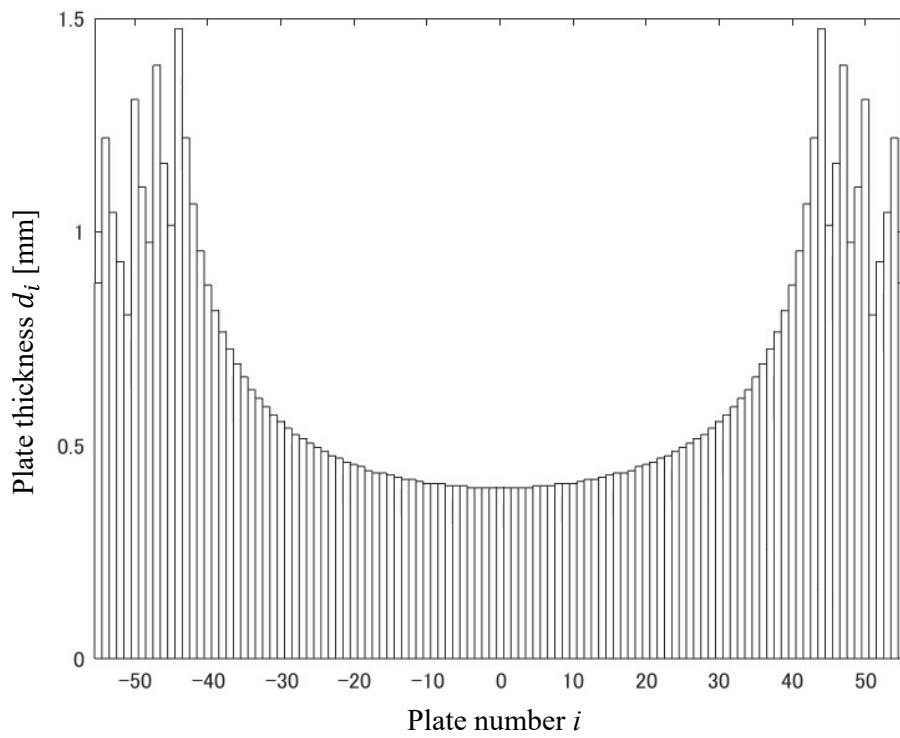


Fig. 4 Thickness combination for transverse wave focusing

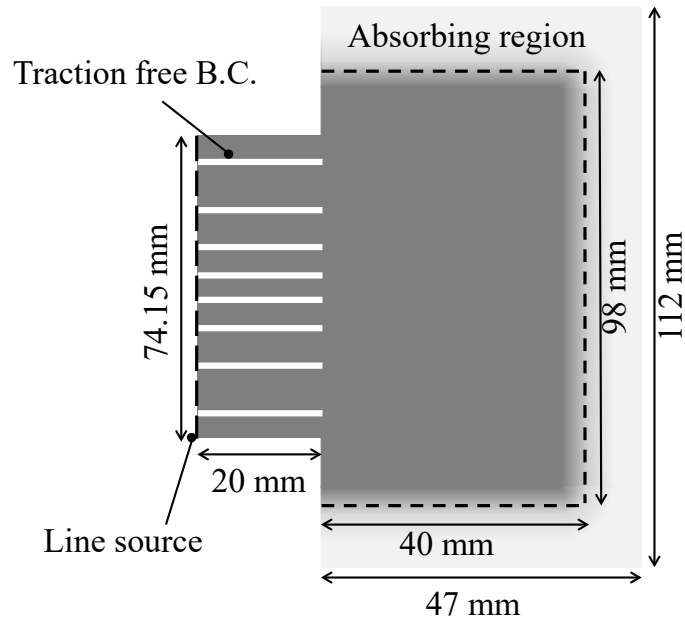


Fig. 5 Calculation region for focusing of transverse wave at the center of the bulk region

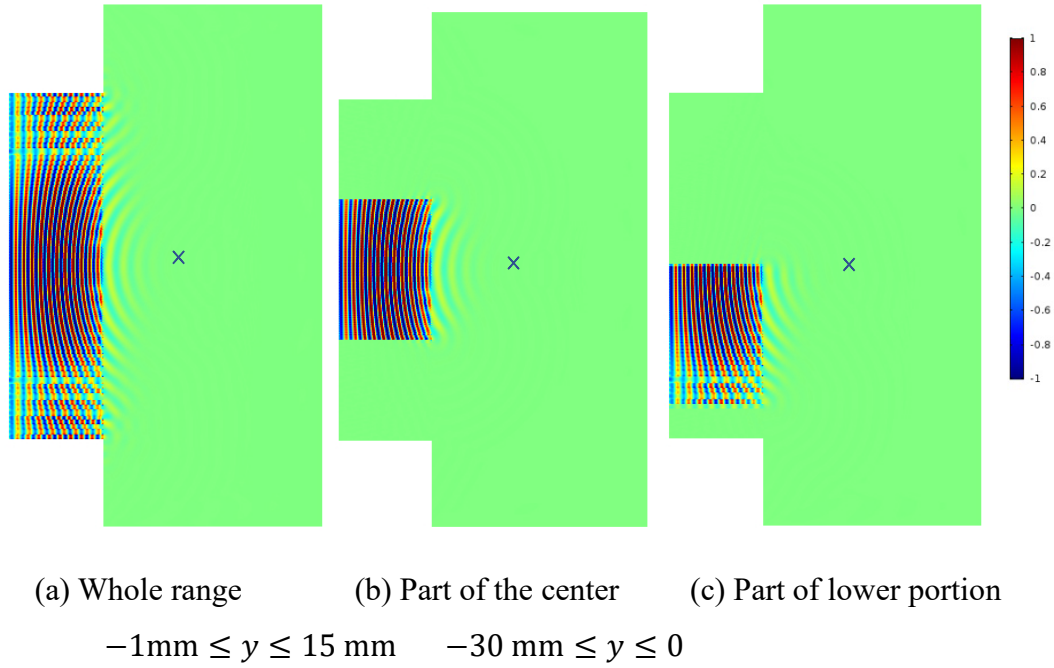


Fig. 6 Wave propagation in a stacked plate region. The surface color is the magnitude of rot \mathbf{u} . The cross mark is the focusing point

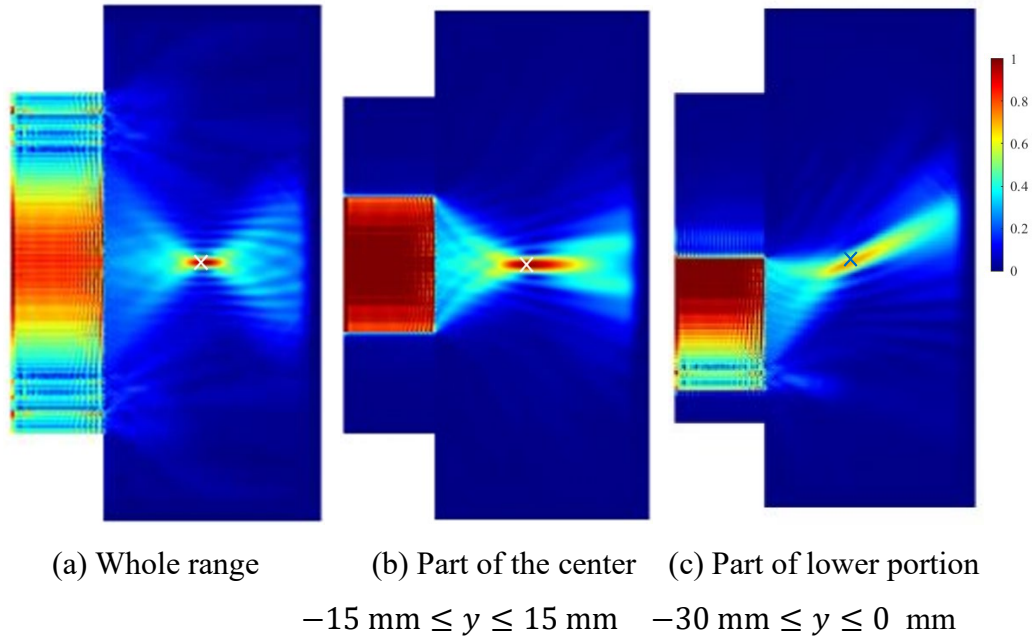


Fig. 7 Wave field for transverse wave focusing with different thickness plates. The color denotes maximum values of $\text{rot } \mathbf{u}$ over the whole time range. The cross mark is a focusing target

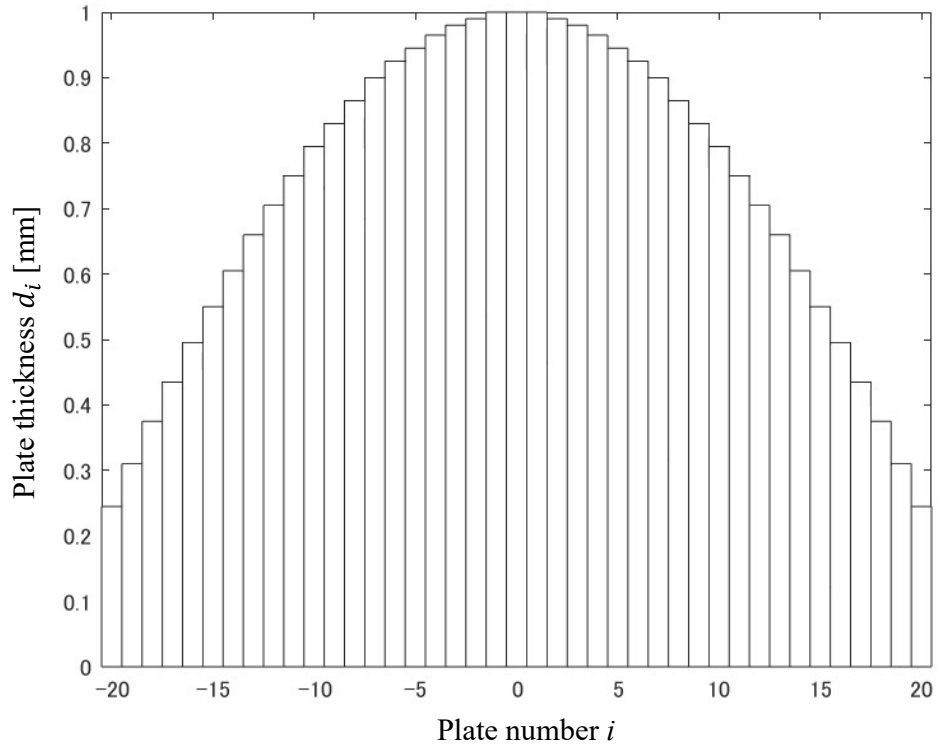


Fig. 8 Thickness combination for longitudinal wave focusing

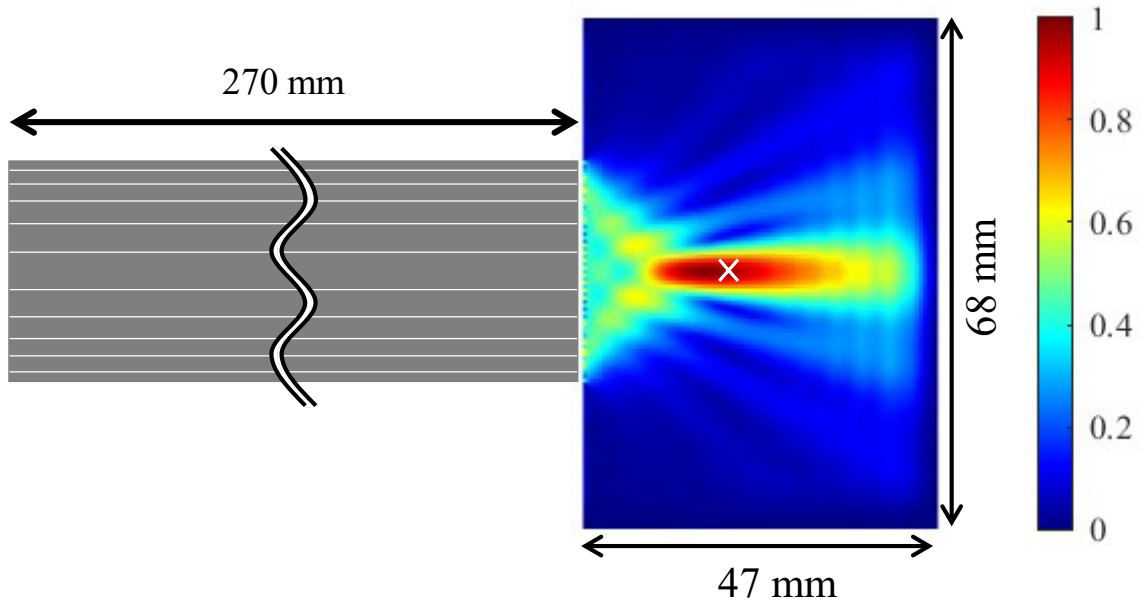


Fig. 9 Wave field for longitudinal wave focusing with different thickness plates. The color denotes maximum values of $\text{div } \mathbf{u}$ over the whole time range. The cross mark is a focusing target

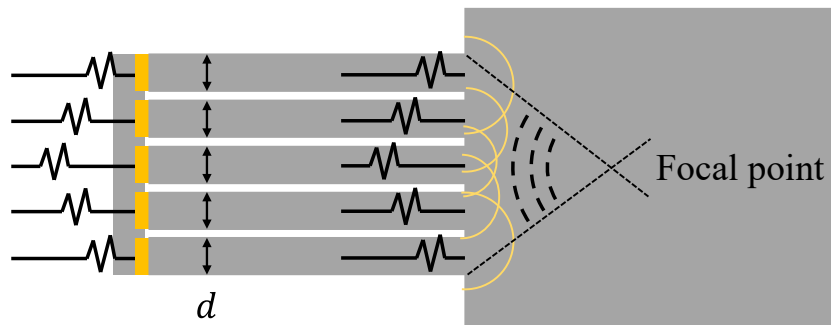


Fig. 10 Ultrasonic focusing using plates with identical thickness and time delay

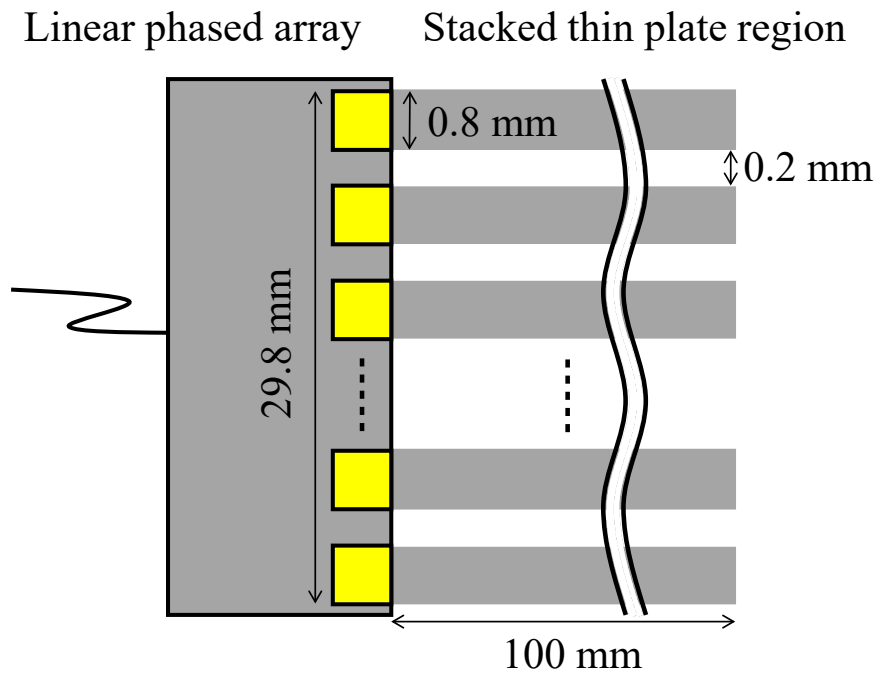


Fig. 11 Relation between linear phased array and stacked plate region

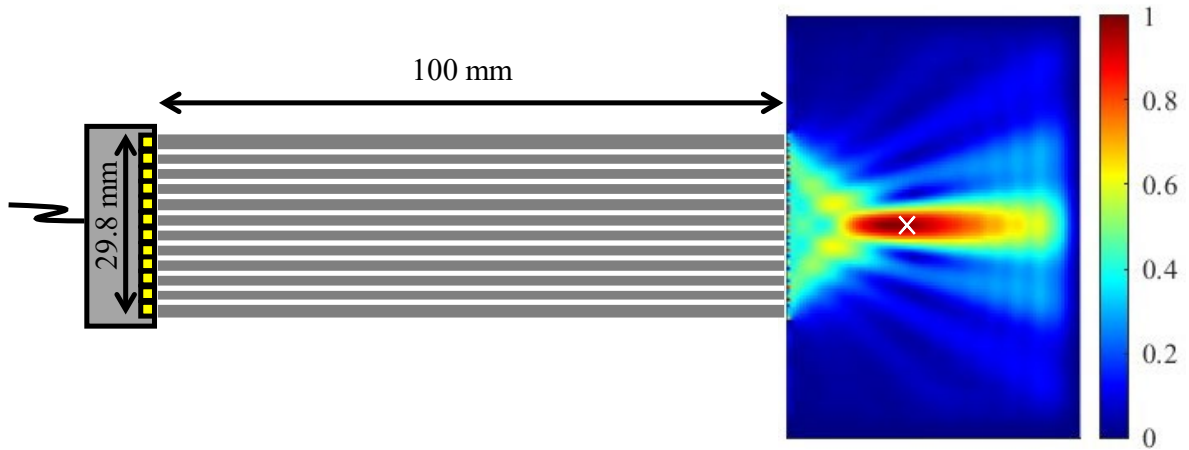
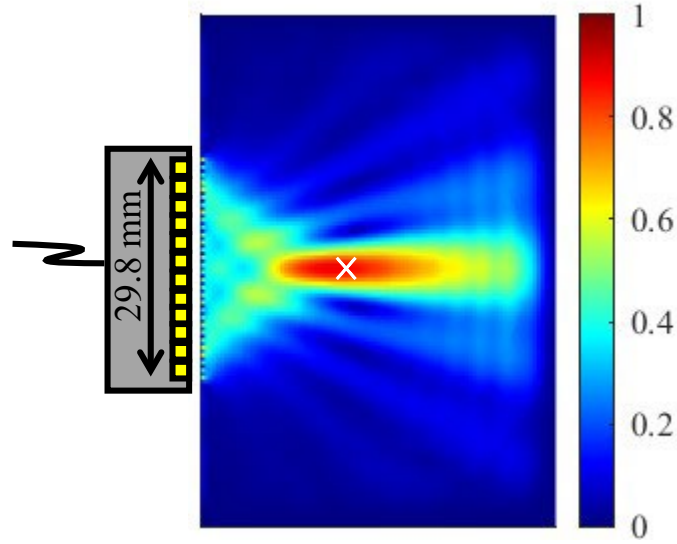
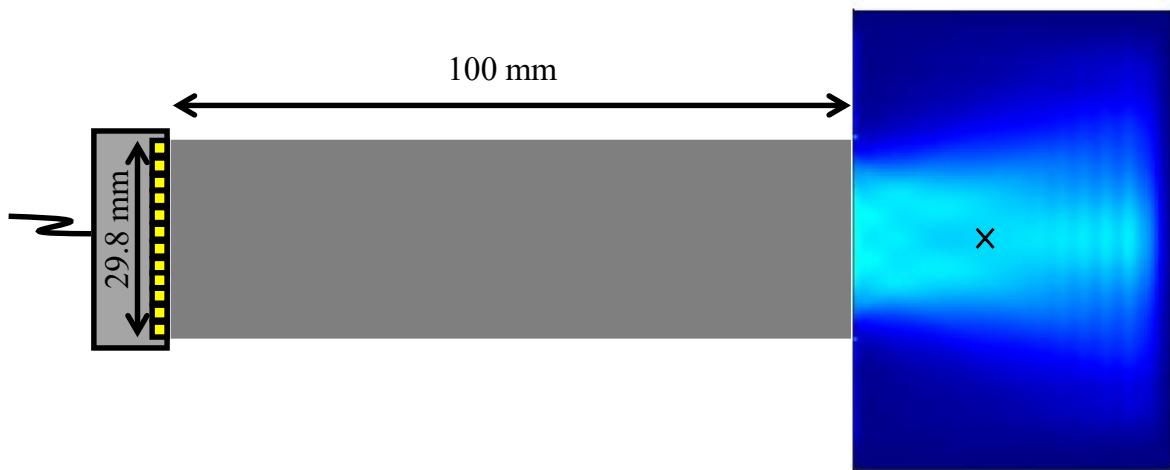


Fig. 12 Wave field for focusing with identical thickness plates and time delayed incident waves. The color denotes maximum values of $\text{div } \mathbf{u}$ over the whole time range

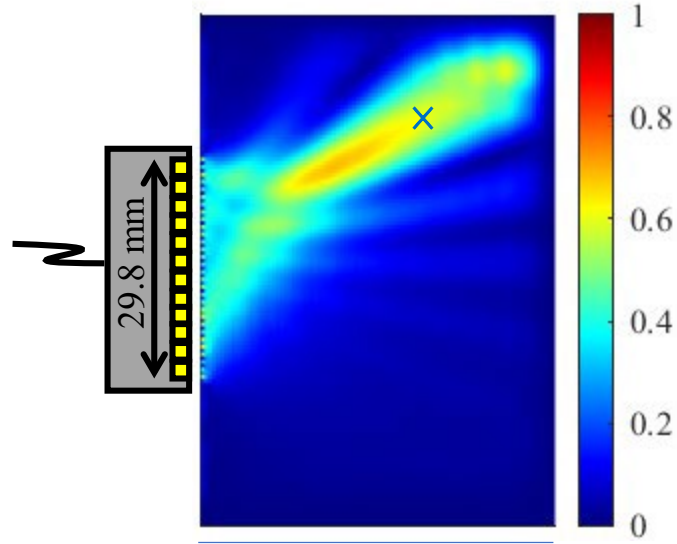


(a) Linear phased array without a buffer material

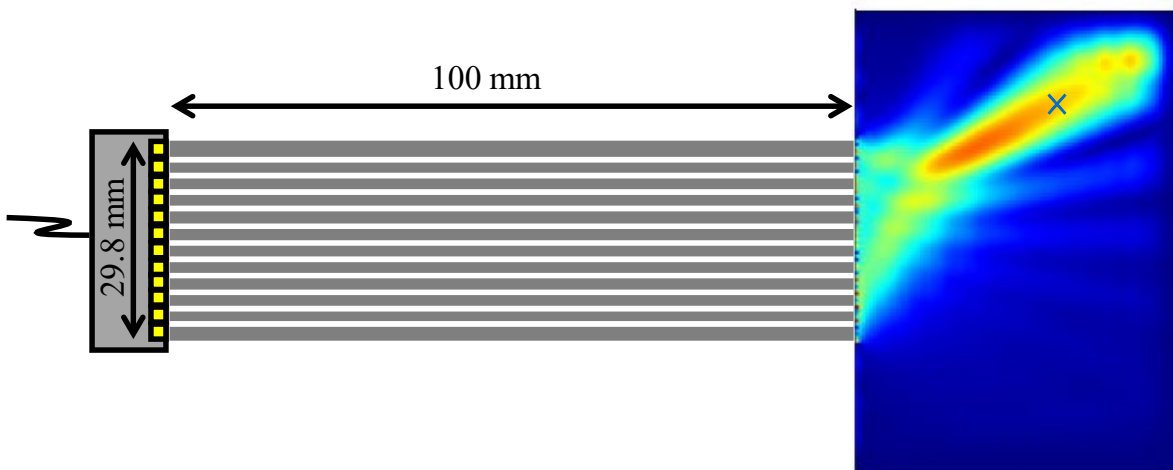


(b) Ordinary buffer material (homogeneous thick plate)

Fig. 13 Wave field for focusing (a) without a buffer material and (b) an ordinary homogeneous buffer material



(a) Linear phased array without a buffer material



(b) With a buffer structure of the stacked plate region

Fig. 14 Wave field for focusing at the off-center of the bulk region